PHOTOGRAMMETRIC INVARIANCE

H. J. THEISS*, E. M. MIKHAIL*, I. M. ALY*, J. S. BETHEL*, C. LEE*
*Purdue University
Geomatics Engineering Department
theiss, mikhail, aly, bethel, changno@ecn.purdue.edu

Working Group III/4

KEY WORDS: Image transfer, Mathematical models, Orientation, Photogrammetry, Reconstruction

ABSTRACT

Two tasks, image transfer and object reconstruction, are investigated using three different approaches. The first approach, based on the fundamental (*F*) matrix, compares the use of all three *F* matrices with epipolar constraints to the use of only two *F* matrices. The second approach uses the four trilinearity equations and employs strategies to deal with the dependency among the equations and the parameters. The third approach is a new one based on collinearity that uses independent equations and therefore yields a rigorous solution.

1 INTRODUCTION

The goal of this research is to investigate and improve invariance techniques to assist in performing photogrammetric tasks. The topics of image transfer and object reconstruction constitute the main sections of this paper. The invariance relationship among image coordinate observations that must be solved to perform image transfer is also a necessary step before doing object reconstruction. Three main approaches – based on the fundamental matrix, the trilinearity equations, and a new collinearity approach – are presented with relevant equations; and results are tabulated for experiments with both simulated and real image data.

2 IMAGE TRANSFER

Image transfer is an application performed on a triplet of images. Given two pairs of measured image coordinates, the third pair can be calculated using a previously established relationship between pairs of image coordinates on all three images. Three basic approaches for establishing the image-to-image relationship are discussed in this paper: the fundamental matrix approach, the trilinearity approach, and the collinearity approach.

2.1 Fundamental Matrix (*F*) Model

The fundamental matrix relates the image coordinates of 3D objects that appear on two images, *i* and *j*, as follows:

$$\begin{bmatrix} x & y & 1 \end{bmatrix}_i F_{ij} \begin{bmatrix} x & y & 1 \end{bmatrix}_j^T = 0 \tag{1}$$

where (x, y) are measured image coordinates.
The 3 by 3 *F* matrix has eight unknown parameters since it is determinable up to a scale factor. In fact there are seven independent parameters, since *F* is of rank two and its determinant must be constrained to equal zero.

Previous techniques based on the *F* matrix have enforced the relationship between only two of the three existing image pairs. In other words, if image coordinates are to be computed on image 3, then we would solve for the elements of only F_{13} and F_{23}. With eight common points between images 1 and 3, we can linearly solve for the eight elements of F_{13} using equation (1). Eight common points between images 2 and 3, which can contain any or all of those used between 1 and 3, can be used in the same way to solve for the elements of F_{23}. The solution can be refined by imposing the determinant equals zero constraint on each of the two *F* matrices, thus reducing the number of independent

unknowns from 16 to 14. For any new 3D object point whose image coordinates are observed in images 1 and 2, the image coordinates of the new point in image 3 are computed by solving two linear equations of the type (1).

In a new F matrix technique, all three possible F matrices are used in a simultaneous, constrained least squares adjustment; see Figure 1. In order to obtain initial estimates for the 24 elements (8 per F matrix), an unconstrained linear solution using at least eight conjugate points per image pair should be performed first. Since the coefficients of the 3 F matrices, i.e. the 24 parameters, are not independent, it is necessary to enforce the epipolar constraint in order to improve the numerical stability and robustness. According to the epipolar constraint, the three pairs of epipoles (e_{12}, e_{13}, e_{21}, e_{23}, e_{31}, and e_{32}) must lie on the same plane that contains the 3 camera stations (C_1, C_2, and C_3) [Faugeras and Papadopoulo, 1997]. See Figure 2.

One form of writing the epipolar constraint equations is in (2a), where e_{23} is the vector of homogeneous coordinates of the epipole on image 2 for C_3, and e_{32} is the epipole vector on image 3 for C_2. Both e_{23} and e_{32} are estimated from F_{23} in Equation (2b):

$$F_{12}e_{23} - F_{13}e_{32} = 0 \tag{2a}$$

$$F_{23}e_{32} = 0, \qquad F_{23}^{T}e_{23} = 0 \tag{2b}$$

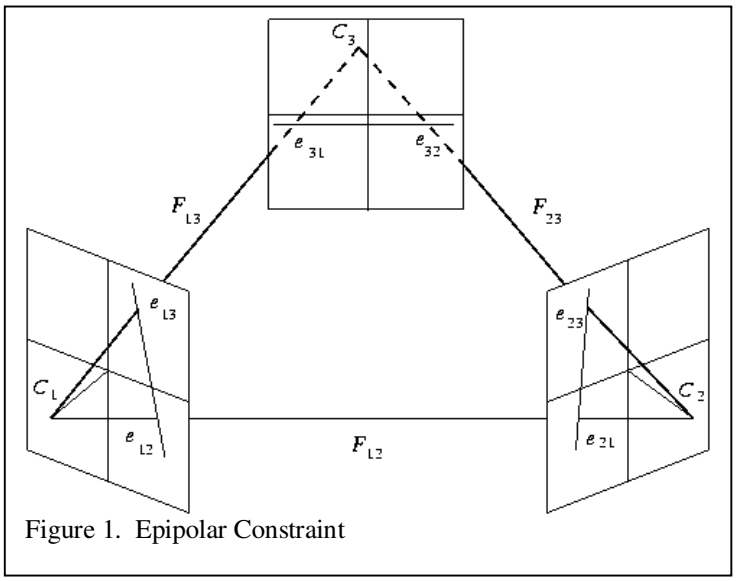

Figure 1. Epipolar Constraint

The three epipolar constraint equations (2a), represented in matrix form, are valid only to a scale factor. Thus we obtain two independent equations from the three by dividing the i^{th} equation by the third equation, for i = 1 and 2 as follows:

$$\frac{F_{12}(i)\begin{bmatrix} e_{x23} \\ e_{y23} \\ 1 \end{bmatrix}}{F_{12}(3)\begin{bmatrix} e_{x23} \\ e_{y23} \\ 1 \end{bmatrix}} - \frac{F_{13}(i)\begin{bmatrix} e_{x32} \\ e_{y32} \\ 1 \end{bmatrix}}{F_{13}(3)\begin{bmatrix} e_{x32} \\ e_{y32} \\ 1 \end{bmatrix}} = 0 \tag{3}$$

where F(i) is the i^{th} 1 by 3 row vector of 3 by 3 matrix F. The two epipolar constraint equations, $G_4 = 0$ and $G_5 = 0$, are obtained for i = 1,2, by clearing fractions in Equation (3). Recall that the first three constraint equations are that the determinants of the F matrices equal zero, or $G_1 = |F_{12}| = 0, G_2 = |F_{13}| = 0, G_3 = |F_{23}| = 0$.

The constraint equations, G_4 and G_5, are written in terms of the epipoles, e_{23} and e_{32}, which are needed to facilitate the writing of the epipolar constraints. These 4 variables, e_{x23}, e_{y23}, e_{x32}, e_{y32}, are called "added parameters" since they are not used as actual parameters in the writing of the condition equations. Since there are four added parameters, we require four additional constraint equations, derived by taking the first two rows of each Equation (2) as follows:

$$G_6 = F_{23}(1)\begin{bmatrix} e_{x32} \\ e_{y32} \\ 1 \end{bmatrix} = 0, \qquad G_7 = F_{23}(2)\begin{bmatrix} e_{x32} \\ e_{y32} \\ 1 \end{bmatrix} = 0, \qquad G_8 = F_{23}^{T}(1)\begin{bmatrix} e_{x23} \\ e_{y23} \\ 1 \end{bmatrix} = 0, \qquad G_9 = F_{23}^{T}(2)\begin{bmatrix} e_{x23} \\ e_{y23} \\ 1 \end{bmatrix} = 0 \tag{4}$$

In summary, for each 3D object point appearing on three images, we write three condition equations of the form of equation (1). A linear solution is implemented to solve for estimates of the F matrix elements that will be used as initial approximations in the next step. Then, a non-linear solution with constraints and added parameters, and the same three condition equations per point, is performed [Mikhail, 1976].

2.2 Trilinearity Model

The geometric relationship between three perspective views is established through the trifocal tensor, which consists of 27 dependent intrinsic elements of a vector *T*. Previous research has shown that the trifocal tensor provides greater immunity to degenerate cases that plague the F matrix techniques for dealing with triplets. Four homogeneous equations that are linear with respect to the elements of *T* can be written as a function of the image coordinates on three overlapping photographs and the 27 elements of *T*. Thus the trifocal tensor can be computed linearly using a set of at least seven points whose image coordinates are measured on all three photographs. Lack of robustness using this linear technique for three-photo image transfer and object reconstruction has prompted us to derive constraints among the 27 dependent elements of *T* to provide stability to the solution, which becomes non-linear due to the constraint equations. An additional constrained solution is provided, which uses only three of the four dependent equations.

2.2.1 Linear Formulation. This subsection provides a summary of the derivation of the four trilinearity equations. The trilinearity equations are derived from the projective relationship that exists between an object point in 3D model space and its associated image coordinates in the 2D image planes of each of the three photographs. Consider the perspective projection for a single photograph. Using projective geometry, a 3 by 4 camera transformation matrix, *P*, linearly relates 3D object coordinates to 2D image coordinates as follows:

$$[x \quad y \quad 1]^T \approx P[X \quad Y \quad Z \quad 1]^T \tag{5}$$

where x,y are image point coordinates,
X,Y,Z are object point coordinates, and
the symbol "$\approx$" implies equality up to a scale factor.

Since we are establishing a relationship between image coordinates, we are not concerned with absolute ground positions of points for now. Therefore, we can assume camera 1 is fixed, and consider the relative positions and orientations of cameras 2 and 3 with respect to the fixed camera 1. Then the relative *P*'s (P_{r1}, P_{r2}, P_{r3}) of the three cameras can be expressed as follows:

$$\underset{3\times4}{P_{r1}} = \left[\underset{3\times3}{I} \;\vdots\; \underset{3\times1}{0}\right], \qquad \underset{3\times4}{P_{r2}} = \{a_{ij}\}, \qquad \underset{3\times4}{P_{r3}} = \{b_{ij}\} \tag{6}$$

These are the matrices that relate the homogeneous model coordinates (X_1, X_2, X_3, t) and the three pairs of image coordinates, (x, y), (x', y'), (x'', y''), on the three images, respectively. The reference [Hartley, 1996] explains why P_{r1} may be assumed, as shown in equation (6), without loss of generality. Note that there are 24 total unknown elements in the three P_r's. Because there is more than one possible value for t, the 24 elements in P_{r1}, P_{r2}, are replaced by a set of 27 dependent *T* coefficients, leading to the following four trilinearity equations (see [Shashua, 1997]):

$$\begin{aligned}
&x''(xT_1 + yT_2 + T_3) - x''x'(xT_4 + yT_5 + T_6) + x'(xT_7 + yT_8 + T_9) - (xT_{10} + yT_{11} + T_{12}) = 0\\
&y''(xT_1 + yT_2 + T_3) - y''x'(xT_4 + yT_5 + T_6) + x'(xT_{13} + yT_{14} + T_{15}) - (xT_{16} + yT_{17} + T_{18}) = 0\\
&x''(xT_{19} + yT_{20} + T_{21}) - x''y'(xT_4 + yT_5 + T_6) + y'(xT_7 + yT_8 + T_9) - (xT_{22} + yT_{23} + T_{24}) = 0\\
&y''(xT_{19} + yT_{20} + T_{21}) - y''y'(xT_4 + yT_5 + T_6) + y'(xT_{13} + yT_{14} + T_{15}) - (xT_{25} + yT_{26} + T_{27}) = 0
\end{aligned} \tag{7}$$

To establish the relationship between image coordinates on a triplet of photographs, we write four equations (7) per point as a function of its six image coordinate observations (x,y,x',y',x'',y'') and 27 trilinearity coefficients (*T*'s), and solve the linear system of homogeneous equations for the 27 parameters. Note that the minimum number of points would be seven, since we would write 28 equations to solve for 27 unknowns.

This linear solution has two problems: 1) although the four equations (7) are linearly independent, only three of the four equations are algebraicly independent [Vieville, et. al., 1993]; and 2) the 27 parameters (*T*'s) are not independent. Therefore, the solution to these linear equations is used to obtain initial estimates for the parameters to be used as input

for one of the nonlinear solutions that contain constraints among the parameters. These refined solutions are discussed in the remaining subsections.

2.2.2 Constrained Solution with Four Dependent Equations (Model 1). There are four constraints among the 27 *T* coefficients in Equations (7) that are commonly used. The first is that the 27th (i.e., the last) element of the vector *T* is set equal to one. The next three are that the determinants of three 3 by 3 matrices, constructed from the *T*'s, are equal to zero; see [Hartley, 1997].

Although this solution with three constraints tends to alleviate some of the instability problems, the solution still is not rigorous because it uses four algebraicly dependent equations. Since it is not possible to linearize with respect to the observations (the corresponding coefficient matrix becomes rank deficient), the objective function to be minimized is the sum of the squared errors of each equation (7) instead of the sum of the squared residuals to the observations.

2.2.3 Constrained Solutions with Three Independent Equations (Models 2,3). There are two models to be discussed that use three independent equations per point. Both of these two models use the first three of the four trilinearity equations; i.e., Equations (7). Since the three condition equations are algebraicly independent, we linearize them with respect to the observations in order to obtain a rigorous solution.

Both models carry 24 parameters with six constraints since there should be only 18 independent parameters. In Model 2, the parameters are 24 of the *T* coefficients (T_1 through T_{24}). In Model 3, however, the values for the elements of P_{r2} and P_{r3} (a_{ij} and b_{ij}) are computed from the initial estimates of the 27 *T* coefficients, and are used as the actual parameters in the adjustment.

The six constraint equations in terms of *T* coefficients are found in [Faugeras and Papadopoulo, 1997]. The six constraint equations in terms of the elements of P_{r2} and P_{r3} are described in [Hartley, 1996]; however, since the reference does not give them explicitly, they are listed below:

$$
\begin{aligned}
G_1 &= a_{11}a_{14} + a_{21}a_{24} + a_{31}a_{34} = 0 \qquad & G_2 &= a_{12}a_{14} + a_{22}a_{24} + a_{32}a_{34} = 0 \\
G_3 &= a_{13}a_{14} + a_{23}a_{24} + a_{33}a_{34} = 0 & G_4 &= \sqrt{a_{14}^2 + a_{24}^2 + a_{34}^2} - 1 = 0 \\
G_5 &= \sqrt{b_{14}^2 + b_{24}^2 + b_{34}^2} - 1 = 0 & G_6 &= b_{33} - 1 = 0
\end{aligned}
\tag{8}
$$

2.3 Collinearity Model (Model 4)

All published derivations to trilinearity use the two scale factors, allow more than one value for *t*, when in theory there should be only one. The following derivation, called "relative collinearity" uses a single scale factor, *t*, and four algebraically independent equations. As in the trilinearity derivation, we compute the 3D projective object coordinates from image 1, and then project the object point into images 2 and 3; see Figure 2. This leads to the following four condition equations:

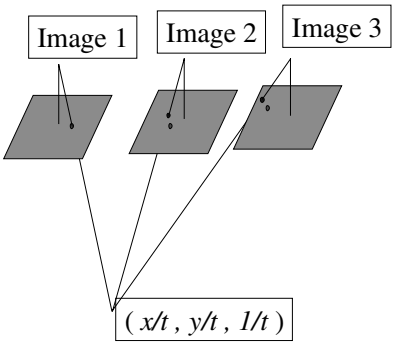

Figure 2. Relative Collinearity Model

$$
\begin{aligned}
F_1 &= x'(a_{31}x + a_{32}y + a_{33} + a_{34}t) - (a_{11}x + a_{12}y + a_{13} + a_{14}t) = 0 \\
F_2 &= y'(a_{31}x + a_{32}y + a_{33} + a_{34}t) - (a_{21}x + a_{22}y + a_{23} + a_{24}t) = 0 \\
F_3 &= x''(b_{31}x + b_{32}y + b_{33} + b_{34}t) - (b_{11}x + b_{12}y + b_{13} + b_{14}t) = 0 \\
F_4 &= y''(b_{31}x + b_{32}y + b_{33} + b_{34}t) - (b_{21}x + b_{22}y + b_{23} + b_{24}t) = 0
\end{aligned}
\tag{9}
$$

These four condition equations are independent; however they contain the additional unknown parameter *t*, which is a unique scale factor for each point observed. The other parameters involved are the 24 total elements of P_{r2} and P_{r3} (a_{ij} and b_{ij}), which are computed from the initial estimates of the 27 *T* coefficients. Note that the *T* coefficients are estimated from the linear solution of the trilinearity equations, (7).

2.4 Experiments

Three data sets are used in the experiments: simulated data with different levels of perturbations; real data over Fort Hood, Texas including 2 near vertical and 1 low oblique aerial frame photographs; and real close range photographs of the EE building on the campus of Purdue University taken with a 75 mm hand-held camera. For each of the data sets, the image transfer process is performed and tested on a triplet of images using each of the methods. First, image coordinate measurements of "control points" on all three photographs are used to solve for the parameters associated with the current method. Then, using those parameters and the measured image coordinates on the first two images of "check points", the conjugate image coordinates on the third image are computed. Finally, the computed and measured image coordinates of the check points on the third image are differenced and collectively expressed as root mean square (RMS).

2.4.1 Simulated Data. Simulated ground points are situated in the range of 0 to 400 meters in X and Y, and between 0 and 125 meters in Z. The ground points are intersected in the image planes of 3 simulated convergent frame photographs with nominal camera station heights of 460 meters and focal lengths of 150 mm. Two photographs are tilted at nominal angles (φ) of 33 degrees, while one photograph is near-vertical. The image coordinates on the three photographs are perturbed with noise of magnitudes 10, 15, and 25 micrometers. The results for all of the discussed image transfer methods are shown in Table 1; note that points are transferred to the near vertical photograph.

Model	10 μm perturbation		15 μm perturbation		25 μm perturbation	
	x RMS (mm)	y RMS (mm)	x RMS (mm)	y RMS (mm)	x RMS (mm)	y RMS (mm)
Model 1	0.013	0.041	0.038	0.055	0.038	0.075
Model 2	0.014	0.049	0.046	0.042	0.044	0.074
Model 3	0.014	0.049	0.046	0.042	0.044	0.074
Model 4	0.014	0.049	0.046	0.042	0.044	0.074
3F's	0.049	0.058	0.056	0.041	0.054	0.073
2F's	0.083	0.139	0.054	0.041	0.206	0.194

Table 1. Image Transfer Experiments with Simulated Data, 8 control points and 7 check points

2.4.2 Fort Hood Data. The Fort Hood data set consists of two near vertical aerial frame photographs taken at 1650 meters above mean terrain, and one low-oblique aerial frame photographs taken at a flying height of 2340 meters with a 25 degree (from the vertical) side-looking angle; see Figure 4. The pixel size for all three photographs is 30 by 30 micrometers. Table 2 shows the results of image transfer to the oblique photograph.

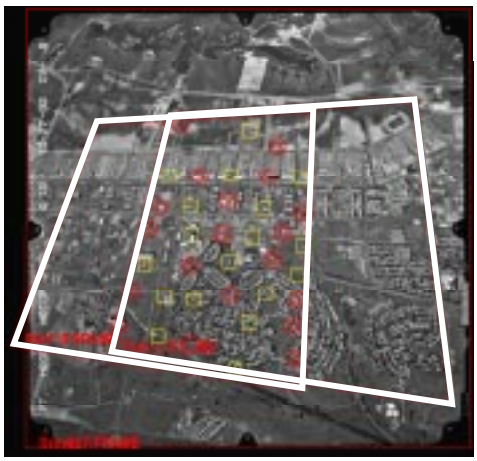

Figure 3. Fort Hood: Footprints of 2 Vertical Aerial Frames Overlaid on 1 Oblique Frame

Model	x RMS (pixels)	y RMS (pixels)
Model 1*	0.64	0.59
Model 2**	0.47	0.61
Model 3**	0.47	0.61
Model 4	0.47	0.61
3F's	0.54	0.62
2F's	0.50	0.62

Table 2. Image Transfer Experiments with Fort Hood Data, 19 control points, 18 check points

* After scaling image coordinates to range from -1 to +1.
** After rotating image coordinates by 90 degrees.

As noted by the asterisks below Table 2, the raw image coordinate data must be augmented for Models 1-3 in order to obtain those results. Since Model 1 does not rigorously linearize with respect to the observations, the image coordinates must be scaled in order to prevent the solution from becoming unstable. A degenerate case occurs for Models 2 and 3 for this particular case of aerial photography where the air base direction between the two near vertical photographs is parallel to the image x coordinate direction and the first three algebraicly independent equations, i.e. Equations (7), are selected.

2.4.3 Purdue EE Building Data. The Purdue EE building data set consists of three convergent photographs taken from a parking garage approximately 30-50 meters away from the Electrical Engineering Building on the Purdue University Campus; see Figure 4. Two pictures were taken from the top level of the garage (43 and 42), while one was taken from ground level (48). Photographs were taken with a 75mm hand-held camera, and the diapositives were scanned at 15 micrometers. The results for image transfer to photograph 48 are shown in Table 3.

Figure 4. Purdue EE Building Data, Frames 43, 42, 48, from left to right

2.4.4 Discussion of Image Transfer Results. Results from these three data sets show that provided that degenerate cases do not exist, Models 2 and 3 will converge and their results will be the same as in Model 4. Thus, for the remainder of the paper results from Models 2-4 will be combined and printed as if the same model. Models 2-4 are rigorous in the sense that they all linearize with respect to the observations, unlike Model 1 which may give unpredictable results.

As for the *F*-matrix technique, the technique that uses all three *F* matrices and their associated constraints is less susceptible to noise, as shown clearly by comparing the last two rows of Table 1 for 25 micrometers of noise. Although not as robust of a technique as collinearity, *F*-matrix techniques have the benefit of being applicable to those parts of the scene where points can be observed on two images only.

Model	x RMS (pixels)	y RMS (pixels)
Model 1	1.48	1.40
Model 2	1.43	1.37
Model 3	1.43	1.37
Model 4	1.43	1.37
3F's	1.29	1.95
2F's	1.24	2.01

Table 3. Image Transfer Experiments with Purdue EE Data, 8 control points, 8 check points

3 OBJECT RECONSTRUCTION

Section 2 described techniques to first establish the relationship between the image coordinates on three photographs. Once the image-to-image relationship is established, the introduction of known 3D control points allows us to solve for the 3D projective transformation matrix. This 4 by 4 matrix is used to transform object points from model to ground coordinates, and similarly to transform the camera transformation matrices from relative to absolute. Therefore, ground coordinates of new points observed on two or more photographs can be computed, and the physical camera parameters can be estimated from the absolute camera transformation matrix.

3.1 3D Projective Transformation Matrix

For the general case of uncalibrated cameras, the model coordinates computed using relative camera transformation matrices are in a 3D non-conformal system that requires a 3D projective transformation to obtain ground coordinates in a 3D conformal system. After the 3D model coordinates have been computed for all of the points, the next step is to compute the 15 elements of the non-singular 4×4 projective transformation matrix, *H*. Since three equations per point can be written, a minimum of 5 points is required to solve for the 15 elements of *H*. (Note that the (4,4) element of *H* is set to unity.) With more than 5 points, a linear least squares solution is applied. The 3D projective transformation *H* is from projective ground space to projective model space. The relations for coordinates and transformation matrices are given by:

$$[X \quad Y \quad Z \quad 1]_r^T \approx H[X \quad Y \quad Z \quad 1]^T \tag{12a}$$

$$P = P_r H$$
$$\underset{3\times4}{P} = \left[\underset{3\times4}{AM} \vdots - \underset{3\times4}{AMS}\right] \qquad (12b\text{-}c)$$

Since Equation (12a) implies equality up to a scale factor, we write three condition equations by dividing each of the first three equations in (12a) by the fourth equation. Once solved for, the *H* matrix may be used as in Equation (12a) to compute absolute ground coordinates, or as in (12b) to compute the absolute camera transformation matrices.

The photogrammetric camera parameters can be extracted from the camera transformation matrix, *P*, in Equation (12c) in which the matrix *A* is a function of x_o, y_o, and *f*, for the standard case of three interior orientation parameters. The matrix *M* is an orthogonal rotation matrix, i.e. a function of three independent rotation angles, ω,φ,κ. *S* is a vector of the three ground coordinates of the camera perspective center, X_L, Y_L, Z_L. The details of an algorithm for extracting camera parameters can be found in [Barakat and Mikhail, 1998] and [Faugeras, 1993].

3.2 Multiple Frame Simultaneous Ground Point Intersection

Following are the two condition equations for each image point on each image, *i*, that are used to solve for the ground coordinates of an object point (*X*, *Y*, *Z*):

$$F_{x_i} = x_i\left(p^i{}_{31}X + p^i{}_{32}Y + p^i{}_{33}Z + p^i{}_{34}\right) - \left(p^i{}_{11}X + p^i{}_{12}Y + p^i{}_{13}Z + p^i{}_{14}\right) = 0$$
$$F_{y_i} = y_i\left(p^i{}_{31}X + p^i{}_{32}Y + p^i{}_{33}Z + p^i{}_{34}\right) - \left(p^i{}_{21}X + p^i{}_{22}Y + p^i{}_{23}Z + p^i{}_{24}\right) = 0 \qquad (13a\text{-}b)$$

where $p^i{}_{jk}$ is the (*j*,*k*) element of the absolute camera transformation matrix for image *i*. An approximate linear solution is obtained by treating the observations and P elements as constants and the object point coordinates as parameters, and using the least squares criterion of minimizing the sum of the squared errors to the equations.

Although some published object reconstruction techniques stop here with the linear solution, we perform a rigorous refinement by linearizing F_x and F_y with respect to parameters and observations. Therefore, we use the general least squares model, $Av + B\Delta = f$; see [Mikhail, 1976].

3.3 Experiments

For each of the data sets in Section 2.4, object reconstruction experiments are run and the results are evaluated by check points. The object reconstruction steps are: 1) establish the relationship between the image coordinates only by solving for the *T* elements or the a_{ij} and b_{ij}, which is also the first step for image transfer; 2) Use a minimum of 5 ground control points and the relationship shown in Equation (12a) to solve for the 15 elements of the 3D projective transformation matrix, *H*; and 3) Compute the check point ground positions using the image coordinates and the absolute camera transformation matrices and compare to their known values. For each of the data sets, results are shown for both the linear solution and the nonlinear refinement. Two-frame versus three-frame ground point intersections are also considered.

Table 4 shows the results from object reconstruction with simulated data, using image coordinates on the two oblique frames to compute the check points. The non-linear refinement does not improve the results for this data set. Models 2-4 show some improvement compared to Model 1.

Method	Model #	10 μm perturbation			15 μm perturbation			25 μm perturbation		
		X RMS (meters)	Y RMS (meters)	Z RMS (meters)	X RMS (meters)	Y RMS (meters)	Z RMS (meters)	X RMS (meters)	Y RMS (meters)	Z RMS (meters)
Linear	1	0.04	0.05	0.11	0.12	0.15	0.20	0.13	0.15	0.23
	2-4	0.14	0.08	0.17	0.13	0.08	0.12	0.14	0.13	0.19
Non-Linear	1	0.04	0.07	0.12	0.12	0.15	0.20	0.13	0.13	0.22
	2-4	0.14	0.08	0.17	0.13	0.07	0.12	0.14	0.13	0.20

Table 4. Object Reconstruction with Simulated Data, 8 control points, 7 check points

Table 5 shows the results of object reconstruction using both real data sets; i.e., Fort Hood and Purdue EE. With Fort Hood, cases are shown with ground point intersections using only the two near vertical frames versus using all three frames simultaneously. There are 19 control points and 18 check points. With the Purdue EE data set, results from intersection of frames 42 and 43 are compared to three frame simultaneous intersection. For this close range data set, there are 8 control points and 8 check points. Note for the Fort Hood data set that the nonlinear refinement offers significant improvement over the linear solution, especially for the three-frame case.

Method	Model #	Fort Hood Data Set						Purdue EE Data Set					
		2 Frame Intersection RMS (meters)			3 Frame Intersection RMS (meters)			2 Frame Intersection RMS (meters)			3 Frame Intersection RMS (meters)		
		X	Y	Z	X	Y	Z	X	Y	Z	X	Y	Z
Linear	1	0.07	0.09	0.17	0.25	0.80	1.24	0.33	3.79	0.51	0.23	2.63	0.35
	2-4	0.06	0.09	0.14	0.12	0.49	0.72	0.16	0.34	0.06	0.15	0.34	0.08
Non-linear	1	0.07	0.09	0.17	0.23	0.20	0.53	0.33	3.79	0.50	0.22	2.62	0.35
	2-4	0.06	0.07	0.14	0.04	0.04	0.09	0.16	0.34	0.06	0.16	0.34	0.08

Table 5. Object Reconstruction with Real Data Sets

4 CONCLUSIONS

Invariance techniques are relatively fast and efficient, and are especially useful for application to imagery obtained from uncalibrated cameras and with unusual geometry. By recognizing photogrammetric implications and applying the necessary constraints, improvements in robustness and accuracy for invariance techniques can be obtained. Although these refined techniques are attractive, the simpler linear techniques can not be abandoned since they provide reasonable initial approximations for the more robust nonlinear techniques. More specifically, it was reinforced that to establish the relationship between image coordinates of a triplet of images, there should be three independent equations per point and 18 independent parameters. Finally, for a rigorous solution to either the image transfer or object reconstruction problem, linearization with respect to the observations is required.

ACKNOWLEDGMENTS

The research presented is sponsored by the U.S. Army Research Office under Grant No. DAAH04-96-1-0444. The views expressed in this paper do not necessarily reflect the views of the U.S. Government or the U.S. Army Research Office.

REFERENCES

[Barakat and Mikhail, 1998]. Barakat, H.F. and Mikhail E.M., "Invariance-supported photogrammetric triangulation", Proceedings of ISPRS Commission III Symposium, vol 32, part 3/1, July, 1998.

[Faugeras, 1993]. Faugeras, O., "Three-dimensional computer vision: a geometric viewpoint", The MIT Press, Cambridge, MA, 1993.

[Vieville, et. al., 1993]. Vieville, T., Navab, N., and Luong, Q.T., "Motion of lines in the uncalibrated case: algebra versus geometry", Technical report, INRIA, fall 1993.

[Faugeras and Papadopoulo, 1997]. Faugeras, O. and Papadopoulo, T., "A nonlinear method for estimating the projective geometry of three views", Technical Report 3221, INRIA, July, 1997.

[Hartley, 1997]. Hartley, R., "Lines and points in three views and the trifocal tensor", International Journal of Computer Vision., v 22, n 2, March, 1997. p 125-140.

[Shashua, 1997]. Shashua, A. "Trilinear tensor: the fundamental construct of multiple-view geometry and its applications", International Workshop on Algebraic Frames For The Perception Action Cycle (AFPAC), Kiel Germany Sep. 8-9, 1997.